

A&A manuscript no.
(will be inserted by hand later)

Your thesaurus codes are:
08(08.12.2; 08.12.3);10(10.07.3)

ASTRONOMY
AND
ASTROPHYSICS

The Mass Function of NGC 288

A. Pasquali¹, M.S. Brigas^{1,2}, and G. De Marchi^{1,3,4}

¹ ESO/ST-ECF, Karl-Schwarzschild-Strasse 2, D-85748 Garching bei München, Germany

² Osservatorio Astronomico di Cagliari, Strada 54, Poggio dei Pini, 09012 Capoterra, Cagliari, Italy

³ STScI, 3700 San Martin Drive, Baltimore, MD 21218, USA

⁴ Affiliated with the Astrophysics Division, Space Science Department of ESA

Abstract. We present NICMOS NIC3 observations of the Galactic globular cluster NGC 288, taken South - East at 2.4 times the cluster's half-light radius in the J and H bands. We have detected the cluster main sequence down to $J \simeq 25$ and $H \simeq 24$. The corresponding luminosity function covers the range $3 < M_H < 9$ and peaks at $M_H \simeq 6.8$. The theoretical tracks of Baraffe et al. (1997) at $[Fe/H] = -1.3$ give a mass function which is best fitted by a log-normal distribution with characteristic mass of $m_c = 0.42 M_\odot$ and a standard deviation $\sigma = 0.35$. This result is fully consistent with the global mass function derived by Paresce & De Marchi (2000) for a sample of 12 globular clusters with very different dynamical histories, thus confirming that near the cluster's half-light radius the mass function appears "undistorted" by evaporation or tidal interactions with the Galaxy and should then reflect the initial mass function.

Key words: stars — luminosity function — mass function — globular clusters

1. Introduction

The Galactic globular cluster NGC 288 is located about one degree away from the South Galactic Pole, in a region of negligible interstellar extinction, $E(B - V) = 0.04$ (Alcaino et al. 1997), and very low contamination by field stars. The cluster is at a distance modulus of $(m - M)_V = 14.7$ and is relatively metal-poor with $[Fe/H] = -1.3$ (Alcaino et al. 1997). Its stellar population is characterized by the presence of blue stragglers and by an anomalous horizontal branch (HB) which is almost entirely composed of stars blue-ward of the instability strip (Alcaino et al. 1997). Such a blue HB may well be induced by the second parameter, although the study of Buonanno et al. (1984) ruled out that the HB anomaly observed in NGC 288 is due to any peculiarity in the cluster's He content, metallicity or age. Buonanno et al. (1984) estimated an age of

16 ± 3 Gyr from the $\Delta m_{(TO-HB)}$ method, whereas Alcaino et al. (1997) have derived 14 ± 2 Gyr from isochrone fitting techniques.

NGC 288 has been observed at infrared wavelengths only by Davidge & Harris (1997), who have acquired 3 min exposures in J and 3 min exposures in K of a central field and 48 min images both in J and K of a region at $140'$ West and South of the cluster core. In this way, Davidge & Harris have resolved the red super-giant branch of the cluster down to the upper main sequence (MS) at $K < 20$ and $0 < J - K < 1$. Their isochrone fitting has been performed with the oxygen-enriched (at $[Fe/H] = -1.26$) tracks of Bergbusch & Vandenberg (1992) and has resulted into an age in excess of 16 Gyr.

In this paper, we present the first NICMOS observations of a field in the outskirts of NGC 288 taken in the J and H bands. The data are described in Section 2 and the cluster's colour-magnitude diagramme (CMD) and mass function (MF) are presented in Section 3. Discussion and conclusions follow in Section 4.

2. Observations and data reduction

NGC 288 has been observed with the NIC3 camera of the NICMOS instrument on board the HST during the parallel observations campaign (GO 7811). The observed region is located 2.4 times the cluster's half-light radius ($r_{hl} = 2'25$; Djorgovski 1993) away from the centre, or $1'6$ E and $5'1$ S. Six images of the same field are available, both in the J and H bands (NIC3 filters F110W and F160W, centered at $1.1 \mu m$ and $1.6 \mu m$, respectively) for a total exposure time of 45 min in J and 47 min in H . The detailed log of the observations is given in Table 1.

The images have been reduced using the NICMOS standard calibration pipeline: they have been first processed with CALNICA for bias subtraction, dark-count correction and flat-fielding. They have then been associated and combined with CALNICB, to remove cosmic rays and to increase the signal-to-noise ratio. Photometry on the images has been performed with the DAOPHOT package. Stars have been identified with DAOFIND, by setting the detection threshold at 10σ above the back-

Send offprint requests to: A. Pasquali

Correspondence to: Anna.Pasquali@eso.org

Table 1. Log of the observations

Image	Filter	Exposure time (s)
N4EZ07CWQ	F110W	575.94
N4EZ07CXQ	F160W	575.94
N4EZ07D1Q	F110W	575.94
N4EZ07D3Q	F160W	575.94
N4EZ08D8Q	F110W	575.94
N4EZ08D9Q	F160W	575.94
N4EZ08DDQ	F110W	575.94
N4EZ08DFQ	F160W	575.94
N4F001CMQ	F110W	191.96
N4F001CNQ	F160W	255.96
N4F001CPQ	F110W	191.96
N4F001CQ	F160W	255.96

ground. We have traced the radial profile of each identified object and discarded those which showed a full width at half-maximum (FWHM) larger than $2''.5$, being the typical FWHM of a point source $1''.5$ in our frames. This procedure has produced a sample of 75 stars. We have also detected 15 extended objects, whose fundamental parameters (flux, position and shape parameters) have been measured with S-Extractor.

The field not being crowded, stellar count-rates have been measured in fixed apertures of 5 pixel radius (equivalent to $1''$), and the corresponding background values have been determined in a fixed annulus with a radius of 7 pixel and a width of 3 pixel. After background subtraction, stellar count-rates have been corrected for the NIC3 intra-pixel sensitivity, using the equations computed by Storrs et al. (1999, cf. Table 2) in the case of out-of-focus campaign data, and for the camera being out of focus, making use of TinyTim (Krist & Hook, 1999) which simulates the PSF of the NIC3 camera with the precise optics settings corresponding to a specific filter and to a specific observation date. We have used TinyTim to compute two PSFs for each frame, one for our observation date (November 1997) and one for January, 15, 1998 when NIC3 was in-focus (in-focus campaigns were carried out in 1998 January and June). We have calculated the encircled energy for a 5 pixel aperture for each PSF and used the flux ratio in-focus to out-of-focus to correct our measured count-rates. Finally, we have multiplied the sample count-rates by a factor of 1.075 to reconvert them to the values measured in a nominal infinite aperture.

The corrected count-rates (c) have been converted into the VEGAMAG photometric system by means of the relation:

$$m = -2.5 \log \left(\frac{cU}{Z} \right)$$

where U is the count-rate/flux conversion factor (known as *inverse sensitivity*) and Z is the flux of a zero-magnitude star in the VEGAMAG system, provided for all

NICMOS filters and VEGAMAG bands by the HST Data Handbook and by the NICMOS Photometry Update (cf. <http://www.stsci.edu/instruments/nicmos>).

The main source of error in our photometry is due to the intra-pixel sensitivity effect, that causes up to 30% flux variations among individual images. With the correction of Storrs et al. (1999) the spread in photometry is reduced to 0.1 mag in J and 0.09 mag in H . We, therefore, assume an uncertainty of 0.1 mag in both the J and H bands.

3. Results

3.1. Photometric completeness

The dereddened ($E(B - V) = 0.04$; Alcaïno et al. 1997) J and H magnitude distributions are shown in Figure 1 for the samples of stars and galaxies identified in the observed NGC 288 field. Stars populate the $\sim 18 < J < \sim 25$ and $\sim 18 < H < \sim 24$ intervals, while galaxies distribute in the $\sim 17 < J < \sim 24$ and $\sim 19 < H < \sim 24$ ranges. The fact that stars and galaxies as faint as J or $H \simeq 24$ have been detected indicates that the cluster field does not contain objects fainter than the 24th mag and, thence, that our star sample is complete. Completeness is also secured by the very low level of field crowding, which allows full object detection by eye.

3.2. The Colour-Magnitude Diagramme

The dereddened CMD of the stars in our sample is plotted in Figure 2. It extends over the H -band magnitude interval $18 - 24$ and the $0.1 < J - H < 1.4$ in colour.

We have superposed on the observed distribution the expected H -band magnitudes and $J - H$ colours as computed for low mass stars at $[Fe/H] = -1.3$ by Baraffe et al. 1997 (solid line). The theoretical track is here scaled by the NGC 288 distance modulus $(m - M)_0 = 14.7$. The IR colours provided by Baraffe et al. have been computed adopting the most recent non-grey model atmospheres and an improved equation of state for low mass stars. The quite good agreement between the observed and the theoretical distributions (within an observational uncertainty of 0.2 mag in colour) confirms that we have indeed detected the lower end of the MS of NGC 288.

Particularly evident in Figure 2 is the change of slope occurring at $H \simeq 20$ and $J - H = 0.8$. This is due to the atmospheric opacity being mostly produced by H_2 molecules for stellar masses lower than $0.5 M_\odot$.

3.3. The luminosity and mass functions

In spite of the limited number of stars in our sample, we have been able to trace the luminosity function (LF) for the observed cluster field, as shown in Figure 3, where the number of stars observed in each 0.5 mag bin is plotted as a function of the H -band magnitude. The LF displays

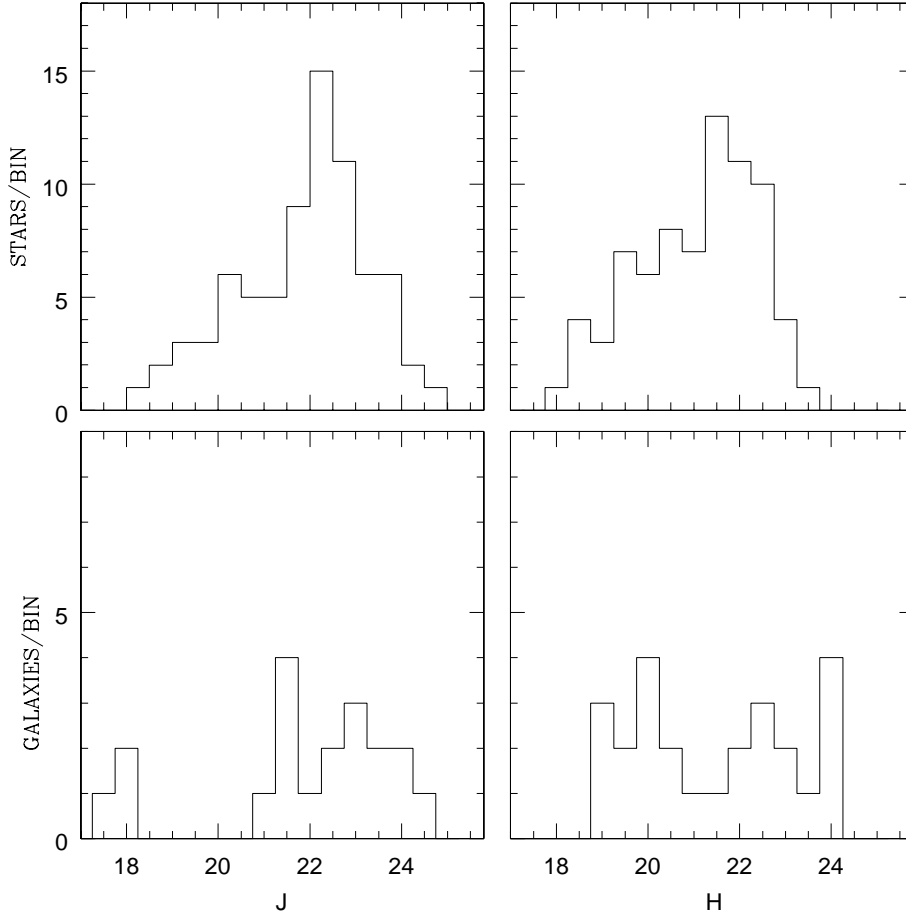


Fig. 1. Magnitude distributions of the star and galaxy samples detected in the observed field

the same general features found by Paresce & De Marchi (2000) for a sample of twelve Galactic globular clusters: a peak at $M_H \simeq 6.8$ (corresponding to $M_I \simeq 8.2$) followed by a rapid decrease towards fainter luminosities.

We have used the mass-luminosity relation corresponding to the theoretical track plotted in Figure 2 to convert the LF into the cluster’s MF. Since the observed LF is the product between the MF and the derivative of the mass-luminosity relation, we have first adopted a specific MF, subsequently derived the mass-luminosity of Baraffe et al. and computed their product. The latter has finally been compared with the observed LF of Figure 3 until a good fit was found. As our first attempt, we have assumed a power-law mass function in the form of $dN/d\log(m) \propto m^{-x}$ (using this notation, Salpeter’s IMF would have $x = 1.35$). We have found, however, that no single power-law mass function can fit the LF of the observed NGC 288 field. Indeed, an index $x = -0.1$ can well reproduce the bright portion of the observed LF at $M_H < 6.8$, but it overestimates the number of stars fainter than the LF peak (cf. top panel of Figure 4). On the other hand, an index $x = -1.1$ properly fits the faint section of the LF at $M_H > 6.8$, but it predicts a number of bright stars a factor of ~ 2 larger than observed (cf. bottom panel of Figure 4).

As an alternative to a power-law, Paresce & De Marchi (2000) have shown that a log-normal distribution peaked at $\sim 0.35 M_\odot$ gives a good fit to the MF of globular clusters for masses smaller than $\sim 0.8 M_\odot$ (i.e. for stars that are still on their MS). Our data show that the LF obtained for MS stars in NGC 288 is fully compatible with a log-normal distribution of the form:

$$\ln \left(\frac{dN}{d\log(m)} \right) = A - \left[\frac{\log(m/m_c)}{\sqrt{2}\sigma} \right]^2$$

where A is a normalization constant, provided that the characteristic mass takes on the value of $m_c = 0.42$ and the standard deviation is $\sigma = 0.35$ (see Figure 5).

We note here, as already pointed out by Paresce & De Marchi (2000), that the fact that a log-normal distribution is a viable form for the MF of a cluster for stars with mass $m < 0.8 M_\odot$ does not imply that the same functional form is appropriate at higher masses as well, where a power-law distribution seems more appropriate (see Elmegreen 1999).

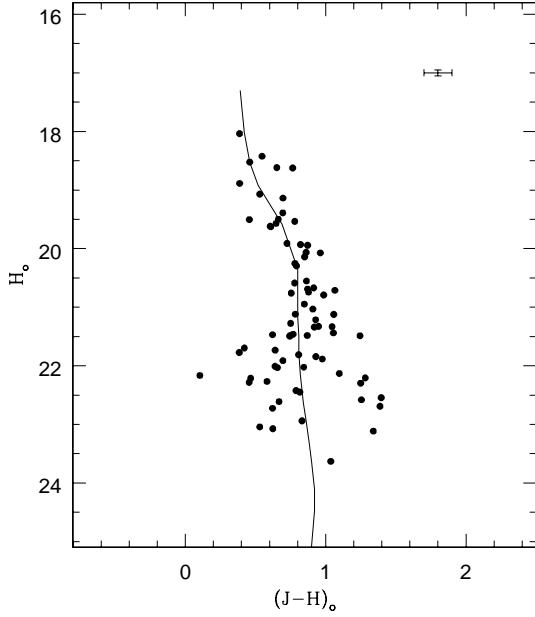


Fig. 2. Dereddened colour-magnitude diagram. The theoretical track of Baraffe et al. (1997) computed for $[Fe/H] = -1.3$ has been superposed to the observed distribution. Uncertainties amount to 0.1 mag and 0.2 mag on H magnitudes and on $J - H$ colours, respectively.

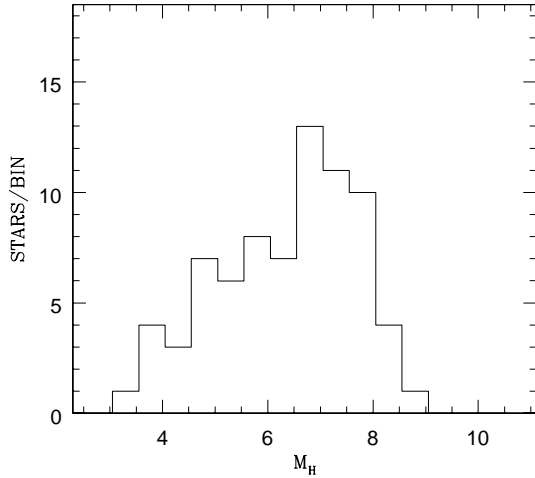


Fig. 3. The luminosity function of the field in the H band. A distance modulus $(m-M)_0 = 14.7$ has been adopted

4. Discussion and conclusions

Comparing the best fitting LF of Figure 5 with the results published by Paresce & De Marchi (2000) indicates that the MF of NGC 288 is fully compatible with the global function found by these authors for a sample of twelve Galactic clusters spanning a wide range of metallicity, different distances from the Galactic centre and plane, and structural parameters (core and half-light radius and concentration ratio).

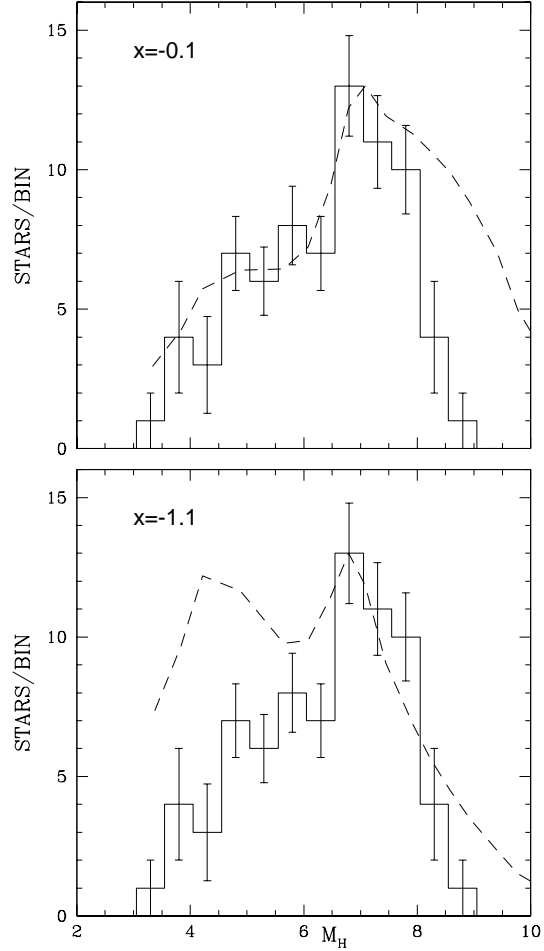


Fig. 4. Two power-law mass functions, $dN/d\log(m) \propto m^{-x}$ have been fitted to reproduce the luminosity function observed for NGC 288. Top panel: an index $x = -0.1$ well matches the bright tail of the LF at $M_H < 6.8$ but fails to reproduce the observed number of fainter stars. Bottom panel: an index $x = -1.1$ fits well the faint tail of the LF at $M_H > 6.8$, yet it overestimates the number of bright stars by nearly a factor of 2

NGC 288 is characterized by a highly elliptical orbit which makes disruption by tidal shocking quite effective and more important than disruption by internal two-body relaxation, according to the calculations of Dinescu et al. (1999). In particular, Gnedin & Ostriker (1997) have derived a disruption time of ~ 1 Gyr for NGC 288, which suggests that this cluster might have experienced a strong interaction with the Galactic tidal field during its lifetime, such that it could be totally dissolved within the next Gyr or so.

Using the log-normal MF determined so far, we have computed the index $\Delta \log N$ defined as the logarithmic ratio between the number of stars with mass $m = m_c = 0.42 M_\odot$ and the number of stars with $m = 0.7 M_\odot$. Paresce & De Marchi (2000) have defined such a parameter in order to quantitatively describe the shape of the

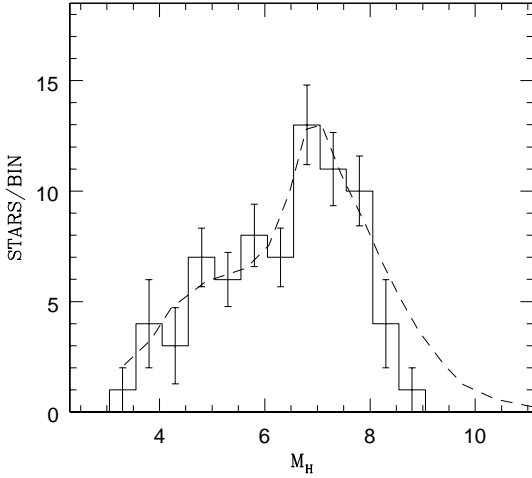


Fig. 5. The best fit to the observed luminosity function is given by the log-normal distribution $\ln(dN/d\log(m)) = A - [\log(m/m_c)/\sqrt{2}\sigma]^2$ where $m_c = 0.42 M_\odot$ and $\sigma = 0.35$

MF and correlate it with the properties of the cluster (see their paper for more details). In Figure 6, we have plotted the value of $\Delta \log N$ for NGC 288 along with those of the clusters studied by Paresce & De Marchi as a function of their expected time to disruption.

We note here that Paresce & De Marchi have measured $\Delta \log N$ on the global MF of the cluster, i.e. the MF after correction of the effects of internal dynamical evolution (mass segregation). The global MF has been shown by De Marchi, Paresce & Pulone (2000) to closely approach the local MF, provided the latter is measured near the cluster's half-light radius (r_{hl}). Our data, however, have been taken at $\sim 2.4 r_{hl}$, so that a correction would be required to our value of $\Delta \log N$ for NGC 288. Unfortunately, we do not have enough data (surface brightness and radial velocity profiles and more than one LF at different radial locations) to investigate the dynamical structure of the cluster and correct for the effects of mass segregation. On the other hand, as shown by De Marchi et al. (2000), at $\sim 2.4 r_{hl}$ the MF is expected to be steeper than the global MF in the mass range of interest here ($0.4 - 0.8 M_\odot$) and, as such, the value of $\Delta \log N$ is to be considered here an upper limit.

Thus, the position of NGC 288 at the opposite corner of NGC 5272 confirms the scattered nature of the distribution in Figure 6, hence the absence of any correlation between dynamical evolution and the MF observed near the clusters half-light radius as pointed out by Paresce & De Marchi. Indeed, compared to the bulk of globular clusters with a mean disruption time $T_d \simeq 32$ Gyr, NGC 288 appears to have suffered the highest degree of erosion from the Galaxy. Yet, its MF is nearly identical to what observed for the cluster sample of Paresce & De Marchi (2000). So, although it has not been determined precisely at the r_{hl} , it is most likely that the observed MF closely reflect the cluster's initial mass function (IMF).

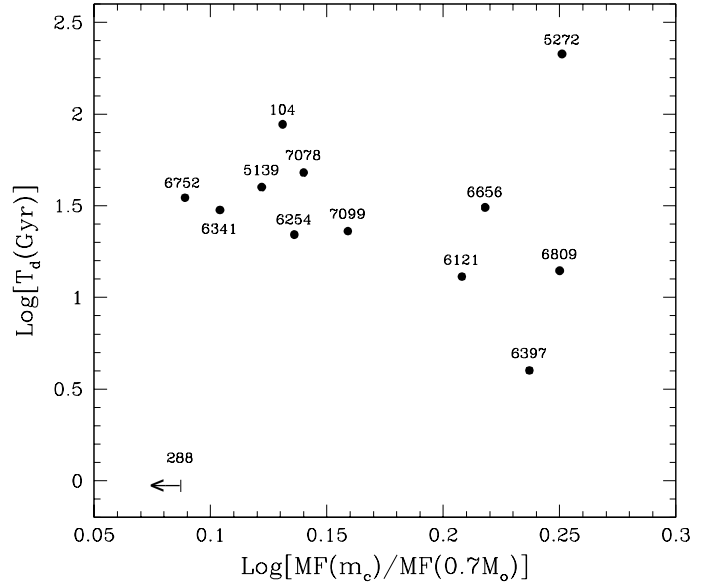


Fig. 6. The plane (Disruption Time) vs. $\log[MF(m_c)/MF(0.7M_\odot)]$ from Paresce & De Marchi (2000) where NGC 288 has been added. The position of NGC 288 (upper limit in $\Delta \log N$) confirms the scattered nature of the distribution so that no correlation between dynamical evolution and mass function may be drawn

An example of the opposite case is offered by NGC 6712, a cluster with a dynamical history not to different from that of NGC 288, yet with a very different MF. Its MF, measured by De Marchi et al. (1999) at $1.7 r_{hl}$ peaks at $0.75 M_\odot$ and slowly drops down to $0.3 M_\odot$, while the average MF of all the clusters in Figure 6 is always increasing in the mass range $0.75 - 0.3 M_\odot$. The lack of low-mass stars (less massive than $0.75 M_\odot$) in NGC 6712 has been attributed by De Marchi et al. (1999) and by Takahashi & Portegies Zwart (2000) to the effect of stripping by tidal interactions with the Galactic bulge.

According to Pryor & Meylan (1993), NGC 288 and NGC 6712 have a concentration ratio of 0.96 and 0.90, respectively, so that they have so far experienced a similar degree of internal two-body relaxation. NGC 6712 is twice more massive but a factor of 4 closer to the Galactic centre. The cluster orbits have the same ellipticity (0.75) but different orbital periods, namely 230×10^6 yr and 130×10^6 yr for NGC 288 and NGC 6712, respectively. Given an apogalactic distance R_a of 11 kpc ($R_p = 1.8$ kpc) and an observed Galactocentric distance $R_{GC} = 11.1$ kpc (Dinescu et al. 1999), NGC 288 is now at its apogalactic point. On the contrary, NGC 6712, with $R_a = 6$ kpc ($R_p = 0.9$ kpc) and $R_{GC} = 3.5$ Kpc, is only half-way between its perigalactic and apogalactic points, so that it has crossed the Galactic bulge more recently than NGC 288. Based on the difference in the orbital phase alone, one might speculate that NGC 288 has been able to thermalize its mass distribution after the bulge shock

while NGC 6712 is still suffering from it. This hypothesis is, however, not applicable as Gnedin & Ostriker (1997) give a relaxation time at half-light radius of 1.4 Gyr and 0.7 Gyr for NGC 288 and NGC 6712, respectively, which is a factor of 5 to 6 larger than the clusters orbital period. Hence, both clusters have still to reach internal relaxation after the last bulge shocking.

Without more data on the LF of these clusters much further out in their periphery, it is not possible to fully understand the differences between their MF. It is, however, plausible that NGC 6712, given its orbital parameters, plunges more deeply than NGC 288 into the bulge so that the low-mass stars depletion observed in its LF is essentially due to stripping by bulge crossing or that the severe modification to its MF has been impressed by encounters with molecular clouds existing in the spiral arms of the Milky Way where this cluster currently sits.

Acknowledgements. We would like to thank Isabelle Baraffe for computing the theoretical tracks at $[Fe/H] = -1.3$ in the NICMOS *J* and *H* bands and Oleg Gnedin for helpful discussions. We also thank an anonymous referee for valuable comments and suggestions that have considerably strengthened the presentation of this work. MSB acknowledges support from the Osservatorio Astronomico di Cagliari and from the Director General's Discretionary Fund at ESO.

References

- Alcaino, G., Liller, W., Alvarado, F., 1997, *AJ*, 114, 2626
 Baraffe, I., Chabrier, G., Allard, F., Hauschildt, P., 1997, *A&A*, 327, 1054
 Bergbusch, P.A., Vandenberg, D.A., 1992, *ApJS*, 81, 163
 Buonanno, R., Corsi, C.E., Fusi Pecci, F., Alcaino, G., Liller, W., 1984, *A&AS*, 57, 75
 Davidge, T.J., Harris, W.E., 1997, *ApJ*, 475, 584
 De Marchi, G., Leibundgut, B., Paresce, F., Pulone, L., 1999, *A&A*, 343, L9
 Djorgovski, S.G., 1993, in *Structure and Dynamics of Globular Clusters*, eds. S.G. Djorgovski & G. Meylan (San Francisco: ASP), p. 373
 Dinescu, D.I., Girard, T.M., van Altena, W.F., 1999, *AJ*, 117, 1792
 Elmegreen, B.G. 1999, *ApJ*, 515, 323
 Gnedin, N.Y., Ostriker, J.P., 1997, *MNRAS*, 289, 927
 Krist, J., Hook, R., 1999, *Tiny-Tim User Guide v5.0*
 Paresce, F., De Marchi, G., 2000, *ApJ*, 534, 870
 Pryor, C., Meylan, G., 1993, in *Structure and Dynamics of Globular Clusters*, eds. S.G. Djorgovski & G. Meylan (San Francisco: ASP), p. 357
 Storrs, A., Hook, R., Stiavelli, M., Hanley, C., Freudling, W., 1999, *NICMOS ISR-99-005*
 Takahashi, K., Portegies Zwart, S. 2000, *ApJ*, 535, 759